A finite-element method using dispersion reduced spline elements for room acoustics simulation

Okuzono, Takeshi

Otsuru, Toru

Tomiku, Reiji

Okamoto, Noriko

(Citation)
Applied Acoustics,79:1-8

(Issue Date)
2014-05

(Resource Type)
journal article

(Version)
Accepted Manuscript

A finite-element method using dispersion reduced spline elements for room acoustics simulation

Takeshi Okuzono[a,1] Toru Otsuru[b], Reiji Tomiku[b], Noriko Okamoto[c]

[a] *Faculty of Engineering, Oita University, 700 Dannoharu, Oita 870-1192, Japan*
[b] *Department of Architecture and Mechatronics, Architecture Course, Faculty of Engineering, Oita University, 700 Dannoharu, Oita 870-1192, Japan*
[c] *Department of Architecture, Ariake National College of Technology, 150 Higashihagio-Machi, Omuta, Fukuoka 836-8585, Japan*

Abstract

This paper presents a finite element method (FEM) using hexahedral 27-node spline acoustic elements (Spl27) with low numerical dispersion for room acoustics simulation in both the frequency and time domains, especially at higher frequencies. Dispersion error analysis in one dimension is performed to increase the accuracy of FEM using Spl27 by modifying the numerical integration points of element stiffness and mass matrices. The basic accuracy and efficiency of the FEM using the improved Spl27, which uses modified integration points, are presented through numerical experiments using benchmark problems in both the frequency and time domains, revealing that FEM using the improved Spl27 in both domains provides more accurate results than the conventional method does, and with fewer degrees of freedom. Moreover, the effectiveness of FEM using the improved Spl27 over that using hexahedral 27-node Lagrange elements is shown for time domain analysis of the sound field in a practical sized room.

Keywords: Room acoustics, Finite element method, Dispersion error, Time domain, Frequency domain

[1] Corresponding author. Tel./fax: +81 97 554 6406/7918.
E-mail address: okuzono@oita-u.ac.jp (T. Okuzono).

1. Introduction

The finite element method (FEM) is a physically reliable numerical method based on wave acoustics for room acoustics simulation in both frequency and time domains[1, 2, 3, 4]. Because FEM is frequently said to be computationally expensive for room acoustics simulation with complex boundary conditions, application of the method is restricted to low-frequency regions in general, but the situation is changing quickly with the rapid progress of computer technology and with the development of efficient methods. Therefore, the use of the method has recently become a realistic option to predict the sound field in an architectural space at the high-frequency region up to some kilohertz.

The authors have developed an efficient FEM[5, 6, 7, 8, 9] using high-order elements, namely, hexahedral 27-node spline acoustic elements (Spl27)[10, 11], preconditioned iterative methods, and parallel computation techniques, to predict large-scale sound fields in rooms with many degrees of freedom (DOF) accurately and efficiently in both frequency and time domains. Here, we define frequency domain FEM and time domain FEM respectively as FD-FEM and TD-FEM. Using the methods, several sound fields in rooms such as concert halls and reverberation chambers have been predicted at low frequencies below one kilohertz, where accuracies were examined by comparison with measurements or other numerical methods[6, 12, 13, 14].

An issue of great concern in finite element (FE) analysis of acoustics is associated with the efficient prediction of sound fields at high frequencies in some kilohertz ranges with reliable accuracy. That issue is reduction of the discretization error, called dispersion error, which is defined as the difference between the exact wave number and numerical wave number or between exact wave velocity and numerical wave velocity. Because of the error, a spatial discretization requirement is imposed in the mesh generation process. For time domain analysis, time discretization error must also be considered in order to yield reliable results. Because these requirements engender a marked increase of computational cost in analysis at high frequencies, many methods have been proposed to reduce the dispersion error[10, 15, 16, 17]. A useful review[15] presents methods for reducing the error in spatial discretization.

Among the methods, there exist a simple but surprisingly efficient method for low-order elements, called modified integration rules (MIR)[16, 18], for reducing the dispersion errors in both frequency and time domain analyses. By simply changing numerical integration points of element matrices from

conventional points in standard FEM using four-node quadrilateral elements, the resulting FEM has fourth order accuracy with respect to dispersion error, whereas standard FEM has second-order accuracy. Therefore, the use of MIR can reduce the computational cost markedly to yield similarly accurate results as the standard FEM with low dispersion error. Recently, we have applied MIR to TD-FEM using hexahedral eight-node elements and an iterative method for room acoustics simulation[19]. The accuracy and efficiency of the TD-FEM using MIR in three dimensions was presented over conventional TD-FEM through three-dimensional dispersion error analysis and numerical experiments, in which we also revealed that the use of MIR improves the convergence of an iterative method to a marked degree.

When modeling sound fields with curved surfaces, discretization of the computational domain using high-order FEs is more efficient than that using first-order FEs such as eight-node hexahedral elements from the perspective of accuracy in geometrical modeling. Furthermore, because the use of the high-order FEs generally produces much more accurate results than first-order FEs does, and with fewer DOF, development of more accurate and efficient FEM using high-order FEs is beneficial to predict sound fields in rooms with complex boundary conditions at high frequencies.

Therefore, the idea of MIR is applied herein to FEM using Spl27 as high-order elements. As a consequence, we propose FEM having improved Spl27 that uses modified integration points in numerical integrations of element matrices based on dispersion relation in one dimension. First, we briefly describe theories of FD-FEM and TD-FEM for sound field analysis and Spl27. Secondly, a method to increase the accuracy of FEM using Spl27, which is based on one-dimensional dispersion relation is presented, particularly addressing reduction of only spatial discretization error. Furthermore, the accuracy in one-dimensional analysis over FEM using conventional spline elements is theoretically estimated as showing the dispersion errors for both methods as a function of spatial resolution. We present the basic accuracy and efficiency of FD-FEM and TD-FEM using the improved Spl27 over conventional method assisted by numerical experiments using benchmark problems in the frequency up to 4 kHz. Finally, the effectiveness of TD-FEM using Spl27 over standard Lagrange elements is demonstrated further.

2. Theory

2.1. FEM for sound field analysis in frequency and time domains

The FE equation in the frequency domain for a three-dimensional sound field (air density, ρ; speed of sound, c) with impedance boundaries and with vibration boundaries, is derived from the principle of minimum potential energy as

$$(\boldsymbol{K} - k^2\boldsymbol{M} + ik\boldsymbol{C})\boldsymbol{p} = i\omega\rho v_{\mathrm{n}}\boldsymbol{W}, \tag{1}$$

where $\boldsymbol{K}$, $\boldsymbol{M}$, and $\boldsymbol{C}$ respectively represent the global stiffness matrix, global mass matrix, and global dissipation matrix. $\boldsymbol{p}$ is the sound pressure vector and $\boldsymbol{W}$ is the distribution vector. k, ω, v_{n} and i respectively denote the wave number, the angular frequency, the velocity of vibration and the imaginary unit. The respective global matrices $\boldsymbol{K}$, $\boldsymbol{M}$, and $\boldsymbol{C}$ are constructed from the respective element matrices defined as follows:

$$\boldsymbol{K}_e = \int_{\Omega_e} \nabla\boldsymbol{N}^{\mathrm{T}}\nabla\boldsymbol{N}d\Omega, \tag{2}$$

$$\boldsymbol{M}_e = \int_{\Omega_e} \boldsymbol{N}^{\mathrm{T}}\boldsymbol{N}d\Omega, \tag{3}$$

$$\boldsymbol{C}_e = \frac{1}{z_{\mathrm{n}}}\int_{\Gamma_e} \boldsymbol{N}^{\mathrm{T}}\boldsymbol{N}d\Gamma, \tag{4}$$

with the normalized acoustic impedance ratio z_{n} and shape function $\boldsymbol{N}$. Ω_e and Γ_e respectively represent the region and surface areas of an element to be integrated. $\boldsymbol{p}$ at an ω is obtainable by solving the linear system of equations of Eq. (1) using a direct method or an iterative method.

FE formulation in the time domain of Eq. (1) can be written as

$$\boldsymbol{M}\ddot{\boldsymbol{p}} + c^2\boldsymbol{K}\boldsymbol{p} + c\boldsymbol{C}\dot{\boldsymbol{p}} = \rho c^2\dot{v}_{\mathrm{n}}\boldsymbol{W}. \tag{5}$$

$\boldsymbol{p}$ in time domain is calculable using a direct time integration method such as Newmark β method[20]. Herein, a method in the Newmark family called Fox–Goodwin method[21] is used for the time integration. The stability condition of the Fox–Goodwin method is given as follows.

$$\Delta t_{\mathrm{crit.}} \leq \frac{1}{\omega_{\max}\sqrt{1/6}}. \tag{6}$$

Therein, $\Delta t_{\mathrm{crit.}}$ is the critical time interval. The maximum natural frequency of system $\omega_{\max}$ is obtainable by solving a generalized eigenvalue problem $(\boldsymbol{K}_e - \omega^2\boldsymbol{M}_e)\boldsymbol{p}_e = 0$. Here, $\boldsymbol{p}_e$ is sound pressure vector within an element.

2.2. Spline acoustic elements

The Spl27[10, 11] is hexahedral 27-node isoparametric FEs using the natural cubic spline polynomial function S_i for $\boldsymbol{N}$. The shape function for Spl27 in three dimensions is defined as

$$\boldsymbol{N}_m(\xi,\eta,\zeta) = S_i(\xi)S_i(\eta)S_i(\zeta) \quad (m = 1, 2, \cdots, 27), \tag{7}$$

with

$$(\text{if} \quad \xi_i = \pm 1) \quad S_i(\xi) = \begin{cases} 0.25\xi^3 + 0.75\xi^2 + 0.5\xi_i\xi & : \xi \in [-1, 0] \\ -0.25\xi^3 + 0.75\xi^2 + 0.5\xi_i\xi & : \xi \in [\ 0, 1] \end{cases} \tag{8}$$

$$(\text{if} \quad \xi_i = \ \ 0) \quad S_i(\xi) = \begin{cases} -0.5\xi^3 - 1.5\xi^2 + 1 & : \xi \in [-1, 0] \\ 0.5\xi^3 - 1.5\xi^2 + 1 & : \xi \in [\ 0, 1] \end{cases} \tag{9}$$

Here, ξ, η, ζ represent the coordinates of a hexahedron in a local coordinate system. ξ_i is the local corner coordinate of the hexahedron in the ξ-direction. For the η-direction and ζ-direction, the function forms of S_i are identical.

3. Dispersion reduced spline acoustic elements

3.1. Dispersion error analysis in one dimension

The method described in **3.2**., which was recently proposed by the authors in a letter[22], uses a dispersion relation in one dimension to increase the accuracy of FEM using Spl27. Here, the dispersion relation between exact wave number k and numerical wave number k^h is derived using a dispersion error analysis in one dimension.

The dispersion error $e_{\text{dis.}}$ is defined as

$$e_{\text{dis.}} = \frac{|k^h - k|}{k}. \tag{10}$$

In the equation presented above, k^h for evaluating $e_{\text{dis.}}$ can be derived analytically, using a FE mesh discretized by three-node spline line elements of nodal distance d, as presented in Fig. 1.

The element matrices $\boldsymbol{K}_e$ and $\boldsymbol{M}_e$ for the three-node spline line elements are calculable using the Gauss-Legendre rules with three numerical integration points as

$$\boldsymbol{K}_e = \sum_{i=1}^{3} W_i \nabla \boldsymbol{N}(\xi_i^K)^{\mathrm{T}} \nabla \boldsymbol{N}(\xi_i^K) \det(\boldsymbol{J}), \tag{11}$$

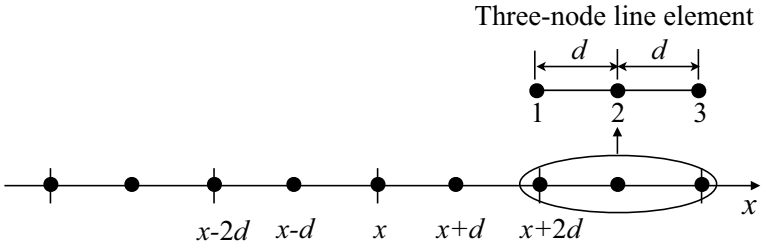

Figure 1: One-dimensional FE mesh used to evaluate dispersion error.

$$\boldsymbol{M}_e = \sum_{i=1}^{3} W_i \boldsymbol{N}(\xi_i^M)^{\mathrm{T}} \boldsymbol{N}(\xi_i^M) \det(\boldsymbol{J}), \tag{12}$$

with a shape function defined as

$$\boldsymbol{N}_m(\xi) = S_i(\xi) \quad (m = 1, 2, 3). \tag{13}$$

Here $\boldsymbol{J}$ represents a Jacobian matrix. W_i, ξ_i^K and ξ_i^M respectively represent the weight and the local coordinates of the i th integration point for $\boldsymbol{K}_e$ and $\boldsymbol{M}_e$. We assume $W_1 = W_3$, $\xi_1^K = -\xi_3^K = -\alpha_K$, $\xi_2^K = 0$, $\xi_1^M = -\xi_3^M = -\alpha_M$, and $\xi_2^M = 0$, considering the symmetry of the integration points.

Neglecting the dissipation term and the source term, the element coefficient matrix ($\boldsymbol{A}_e = \boldsymbol{K}_e - k^2 \boldsymbol{M}_e$) of Eq. (1) with three-node spline elements is given as

$$\boldsymbol{A}_e = \begin{bmatrix} a_{11} & a_{12} & a_{13} \\ & a_{22} & a_{12} \\ \text{sym.} & & a_{11} \end{bmatrix}, \tag{14}$$

where

$$a_{11} = \frac{W_1[4 + 9\alpha_K^2(\alpha_K - 2)^2] + 2W_2}{8d} - \frac{k^2 d W_1 \alpha_M^2[4 + \alpha_M^2(\alpha_M - 3)^2]}{8}, \tag{15}$$

$$a_{12} = \frac{-9W_1\alpha_K^2(\alpha_K - 2)^2}{4d} + \frac{k^2 d W_1 \alpha_M^2[(\alpha_M^2 - 2\alpha_M - 2)(\alpha_M - 3)(\alpha_M - 1)]}{4}, \tag{16}$$

$$a_{13} = \frac{W_1[-4 + 9\alpha_K^2(\alpha_K - 2)^2] - 2W_2}{8d} - \frac{k^2 d W_1 \alpha_M^2[-4 + \alpha_M^2(\alpha_M - 3)^2]}{8}, \tag{17}$$

$$a_{22} = \frac{9W_1\alpha_K^2(\alpha_K - 2)^2}{2d} - \frac{k^2 d[W_1(2 + \alpha_M^2(\alpha_M - 3))^2 + 2W_2]}{2}. \tag{18}$$

Furthermore, FE solutions at node x in free space are given as

$$p_x^h = \mathrm{e}^{ik^h x}. \tag{19}$$

The FE equation at a node x is

$$a_{13}(p_{x-2d}^h + p_{x+2d}^h) + a_{12}(p_{x-d}^h + p_{x+d}^h) + 2a_{11}p_x^h = 0. \tag{20}$$

Similarly, FE equations at nodes $x - d$ and $x + d$ respectively denote

$$a_{12}p_{x-2d}^h + a_{22}p_{x-d}^h + a_{12}p_x^h = 0, \tag{21}$$

$$a_{12}p_x^h + a_{22}p_{x+d}^h + a_{12}p_{x+2d}^h = 0. \tag{22}$$

Combining Eqs. (20)–(22) and substitution of Eq. (19) into the resulting equation yields

$$a_{13}\cos(2k^h d) + a_{11} - \frac{a_{12}^2}{a_{22}}[1 + \cos(2k^h d)] = 0. \tag{23}$$

After simplification, we obtain the numerical wave number k^h as

$$k^h = \frac{1}{2d}\cos^{-1}\left(\frac{-a_{11} + \frac{a_{12}^2}{a_{22}}}{a_{13} - \frac{a_{12}^2}{a_{22}}}\right). \tag{24}$$

From the equation presented above, numerical wave number for three-node spline line elements can be evaluated. For three-node spline line elements using conventional Gauss-Legendre rules ($\alpha_K = \alpha_M = \sqrt{3/5}$, $W_1 = 5/9$ and $W_2 = 8/9$), the k^h is given as

$$k^h = \frac{1}{2d}\cos^{-1}\left[\frac{3105 - 540\sqrt{15} - 6(762 - 119\sqrt{15})(kd)^2 + (336 - 22\sqrt{15})(kd)^4}{3105 - 540\sqrt{15} + 6(273 - 61\sqrt{15})(kd)^2 - (48 - 26\sqrt{15})(kd)^4}\right]. \tag{25}$$

Using the equation presented above, $e_{\mathrm{dis.}}$ for conventional three-node spline line elements is evaluated as $|k^h - k|/k$.

3.2. Numerical integration points for reducing dispersion error

A method for increasing the accuracy of FEM using Spl27 described here uses the dispersion relation of Eq. (24) in which the numerical integration points α_K and α_M of element stiffness and mass matrices are modified from

conventional integration points. The modified integration points can be derived from a condition that minimizes the dispersion error at an arbitrary nondimensional wave number kd on one-dimensional mesh. More specifically the numerical integration points α_K and α_M that satisfy $k^h = k$ in Eq. (24) are calculated under the assumption that $\alpha_K = \alpha_M$, and the calculated integration points are used in calculation of element matrices by Eqs (2) and (3) instead of using the conventional values. For simplicity, weights for i-th integration points use conventional values, i.e., $W_1 = W_3 = 5/9$ and $W_2 = 8/9$. Although the dispersion error appears as the coupling of spatial and time discretization errors in time-domain analysis, the method presented here deals with reduction only of spatial discretization error.

3.3. Comparison of dispersion error in dispersion-reduced spline elements with that in conventional spline elements

The dispersion error in FD-FEM using improved three-node spline line elements that use modified integration points is theoretically evaluated using Eq. (24) and compared with that in FD-FEM using conventional spline line elements, to demonstrate the effectiveness. For the improved spline elements, three modified integration points were designed: α_K=α_M=0.8700, 0.8669, and 0.8558. These were derived from the conditions that minimize the dispersion error at kd corresponding to λ/d=4.8, 5.5, and 6.8, where λ is the wavelength of the upper limit frequency. The other integration points are derived from each condition, but the presented integration points are the most effective values.

Figure 2 presents a comparison of dispersion errors in FD-FEM using the improved spline elements that use three modified integration points and using conventional spline elements, as a function of spatial resolution of mesh. As expected, dispersion errors for FD-FEM using the improved spline elements are minimized at the corresponding λ/d and significant error reductions achieved around λ/d. The theoretically evaluated results clearly showed the effectiveness of FD-FEM using the improved spline elements over conventional methods with smaller dispersion error in one dimension.

4. Numerical examination of the basic accuracy and efficiency of an improved method using benchmark problems

The method described in the previous section modifies numerical integration points based on one-dimensional dispersion error analysis. Therefore,

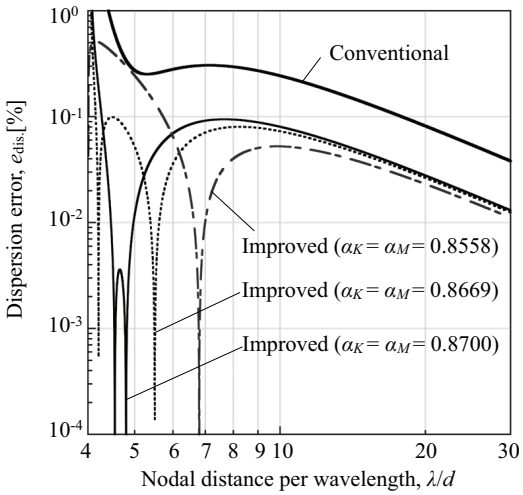

Figure 2: Comparison of dispersion errors as a function of spatial resolution for conventional and improved spline elements.

the effectiveness in three-dimensional analysis remains unclear. This section presents the basic accuracy and efficiency of FEM using Spl27, which uses modified integration points based on one-dimensional dispersion error analysis through the numerical experiments in both frequency and time domains.

For the investigations, two problems, B0-1F Task B and B0-1T Task A, of the benchmark platform on computational methods for architectural / environmental acoustics[23] were selected. These are the problems of computing frequency response or transient response at three receiving points R2, R3, and R4 inside a cubic cavity of 1.0 m^3 (Fig. 3) with rigid boundaries. In the problems, c=343.7 m/s and ρ=1.205 kg/m^3 were respectively assumed.

Three FE meshes with different spatial resolutions were used. The respective values of λ/d are 4.29, 5.16 and 6.0 at 4 kHz. The respective corresponding DOFs are 132,651, 226,981, and 357,911. An iterative method, namely, Conjugate Gradient Conjugate Orthogonal (COCG) method[24] with absolute diagonal scaling as a preconditioning was used to solve the linear system of equations at each frequency in FD-FEM or at each time step in TD-FEM. The convergence tolerance used for the stopping criterion was 10^{-6}. For improved Spl27, three modified integration points derived in the previous section were again used, i.e., α_K=α_M=0.8700, 0.8669, and 0.8558.

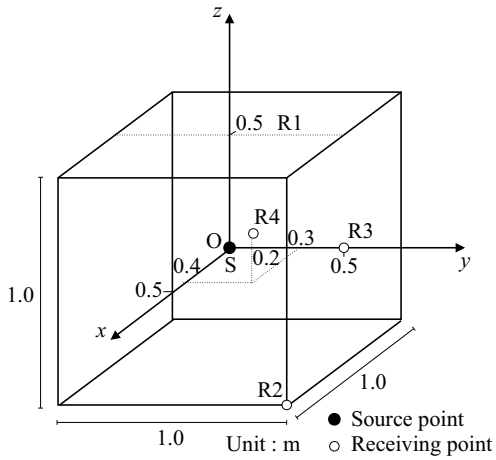

Figure 3: Cubic cavity to be analyzed with a point source S and three receiving points R2, R3, and R4 in the benchmark problems, B0-1F and B0-1T.

4.1. Frequency domain analysis

Sound pressures calculated using FD-FEM with the improved Spl27 and using the conventional Spl27 were respectively compared with those calculated using modal summation method (MS) at frequencies of 20 Hz to 4 kHz with 1 Hz interval. As a sound source, the volume acceleration $i\omega v_{\mathrm{n}}$=1.0 $\mathrm{m}^3/\mathrm{s}^2$ was given at source point S in each frequency.

Figure 4 presents comparisons of relative sound pressure levels of R2 at higher frequencies of 3 kHz to 4 kHz calculated using MS and FD-FEM using conventional Spl27 and improved Spl27(α_K=α_M=0.8700) for most coarse mesh with λ/d=4.29. The agreement of frequencies, at which peaks and dips occur, is much better between MS and FD-FEM using improved Spl27 than that using conventional Spl27, which means that dispersion error can be reduced effectively by FD-FEM using improved Spl27 in three-dimensional analysis.

Although quantitative estimation of accuracy in sound pressure at frequencies having peak value between MS and FEM is difficult for this problem because all boundaries of the room have infinite acoustic impedance, we simply calculated the following error in sound pressure level between modal summation method and FD-FEM using conventional and improved Spl27 at

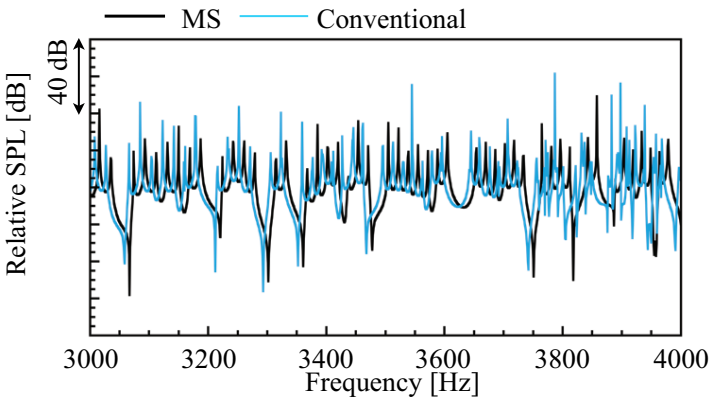

(a) Modal summation method vs. FD-FEM using conventional Spl27

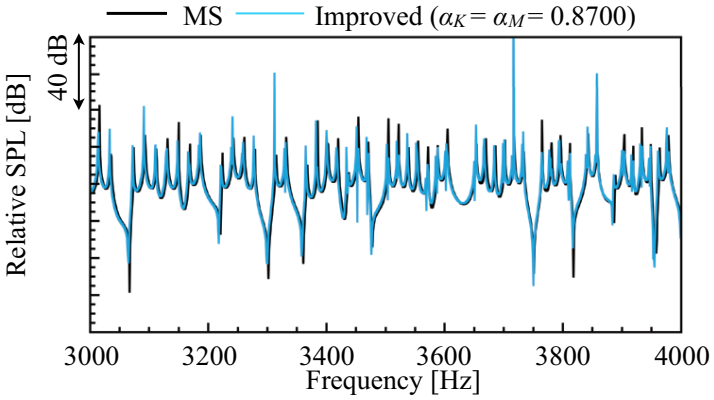

(b) Modal summation method vs. FD-FEM using improved Spl27 (α_K= α_M= 0.8700)

Figure 4: Relative sound pressure levels at a receiving point R2 in frequencies of 3 kHz to 4 kHz for FE mesh with λ/d=4.29: (a) MS vs. FD-FEM using conventional Spl27 and (b) MS vs. FD-FEM using improved Spl27 (α_K=α_M=0.8700).

frequencies of 20 Hz to 4 kHz:

$$e_{\mathrm{L}} = \frac{1}{N_{\mathrm{f}}} \sum_{j=1}^{N_{\mathrm{f}}} e(f_j), \tag{21}$$

with

$$e(f) = \sqrt{\frac{1}{N} \frac{\sum_{i=1}^{N} [L_{\mathrm{MSM}}(\boldsymbol{x}_i, f) - L_{\mathrm{FEM}}(\boldsymbol{x}_i, f)]^2}{\sum_{i=1}^{N} L_{\mathrm{MSM}}(\boldsymbol{x}_i, f)^2}}, \tag{22}$$

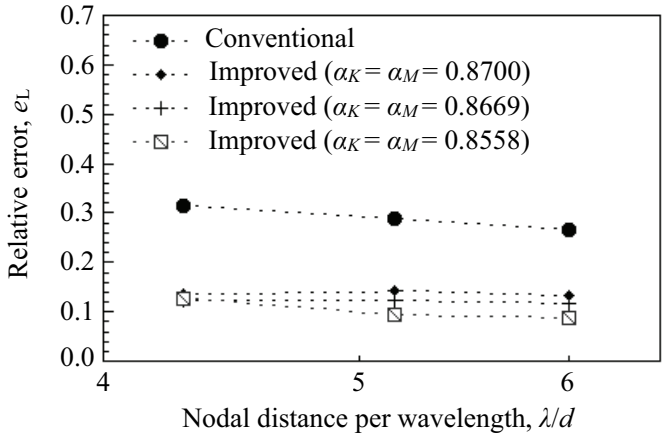

Figure 5: Comparison of relative errors in sound pressure level as a function of spatial resolutions for FD-FEM using conventional Spl27 and using the improved Spl27.

where N_f and N respectively represent the number of frequencies and the number of receiving points. $L_\mathrm{MSM}(\boldsymbol{x}_i, f)$ and $L_\mathrm{FEM}(\boldsymbol{x}_i, f)$ respectively represent the sound pressure level of frequency f at receiving point $\boldsymbol{x}_i$ calculated using modal summation method and FD-FEM using conventional and improved Spl27. Figure 5 presents results for all meshes. Results show that the errors in FD-FEM using improved Spl27 were reduced to 1/2.0–1/3.1 of those in FD-FEM using conventional Spl27.

Furthermore, the convergence property of COCG method must be explained from the perspective of computational efficiency. Figure 6 shows a comparison of the mean iteration number of COCG method at frequencies of 20 Hz to 4 kHz. The use of the improved Spl27 engenders a slight increase of iteration number for convergence, but the increase amounts to only 1.09 times the number in the use of conventional Spl27 at maximum. It can be considered that the increase of iteration number using the improved Spl27 is not significant compared to that of operation using finer FE mesh.

The numerical evidences in accuracy and convergence property clearly showed the effectiveness of FD-FEM using improved Spl27 that uses modified integration points based on one-dimensional dispersion error analysis for three-dimensional analysis.

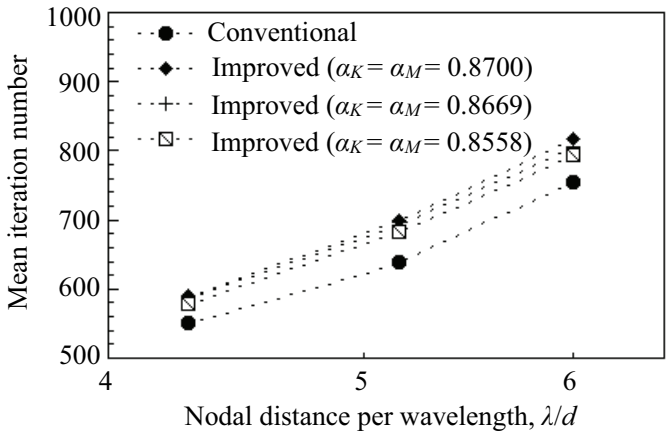

Figure 6: Comparison of mean iteration number of FD-FEM using conventional Spl27 and using the improved Spl27 for FE meshes with different spatial resolutions.

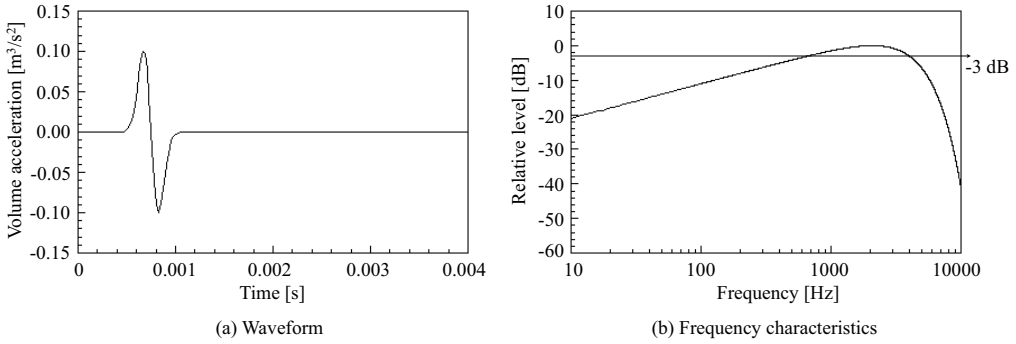

Figure 7: Waveform of a modulated Gaussian pulse for sound source and its frequency characteristics (a) waveform. (b) frequency characteristics.

4.2. Time domain analysis

The sound pressures calculated using TD-FEM with the improved Spl27 and using the conventional Spl27 were, respectively, compared with analytical solution calculated using an analytical method (method of variable separation) with Gaussian pulse[25]. Here, the upper limit frequency was assumed as 4 kHz. A modulated Gaussian pulse was given at source point S as a volume acceleration waveform. Its waveform and frequency characteristics are given in Fig. 7.

The sound pressure was calculated up to 50 ms with the time interval Δt = 1/48,000 s for TD-FEM using improved Spl27 and with Δt = 1/55,000 s

for conventional Spl27, respectively. These Δt's were determined to satisfy the stability condition of Eq. (6) for FE mesh with λ/d=6.0. For TD-FEM using improved Spl27 that uses three modified integration points, the critical time intervals are, respectively, 1/46,682 s (α_K=α_M=0.8700), 1/46,909 s (α_K=α_M=0.8669) and 1/47,738 s (α_K=α_M=0.8558). The value for conventional method is 1/54,421 s. Here, the stability condition was relaxed using modified integration points. Approximately 1.14∼1.17 times larger Δt can be used for the presented modified integration points. To confirm the relaxation theoretically, as an example, $\omega_{\max}$ in the stability condition of Eq. (6) for one-dimensional analysis using three-node spline elements is given as

$$\omega_{\max} = \max\left[\frac{3c}{\sqrt{5}d\alpha_M}, \frac{9c\alpha_K(\alpha_K-2)}{2d\alpha_M^2(\alpha_M-3)}\right]. \tag{26}$$

From the equation above, the $\omega_{\max}$ depends clearly on α_K and α_M, and the relaxation of the stability condition for improved method can be found, substituting conventional and modified integration points into Eq. (26), respectively. Although this relaxation in low-order four-node quadrilateral and eight-node hexahedral FEs for two and three-dimensional analyses has been pointed out[16, 19], we newly revealed here the effect for the high-order spline elements.

Figure 8 presents comparisons of sound pressures at R3 calculated using the analytical method and TD-FEM using conventional Spl27 and improved Spl27 (α_K=α_M=0.8669) for most coarse mesh with λ/d=4.29. The fine structure of sound pressure calculated using TD-FEM using the improved Spl27 agrees well with analytical solution, and the agreement is much better than that between TD-FEM using conventional Spl27 and analytical method, with smaller numerical oscillation. As shown in Fig. 9, the small oscillation in sound pressure calculated using TD-FEM using the improved Spl27 disperse for finer mesh with λ/d=6.0, whereas the oscillation can still be observed in sound pressure after the first reflection calculated using TD-FEM using conventional Spl27.

For quantitative estimation of accuracy in TD-FEM using improved Spl27, the relative error in sound pressure between analytical method and TD-FEM using conventional and improved Spl27 was calculated as

$$e_{\mathrm{p}} = \frac{1}{N_{\mathrm{step}}}\sum_{j=1}^{N_{\mathrm{step}}} e(t_j), \tag{27}$$

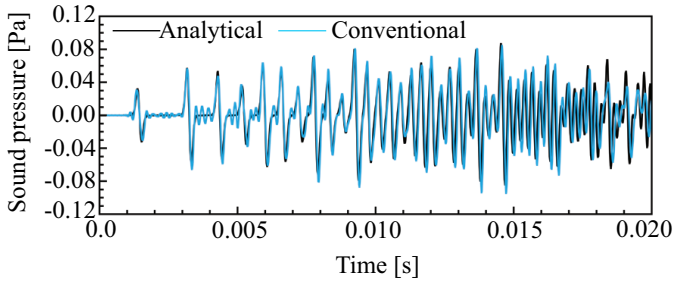

(a) Analytical method vs. TD-FEM using conventional Spl27

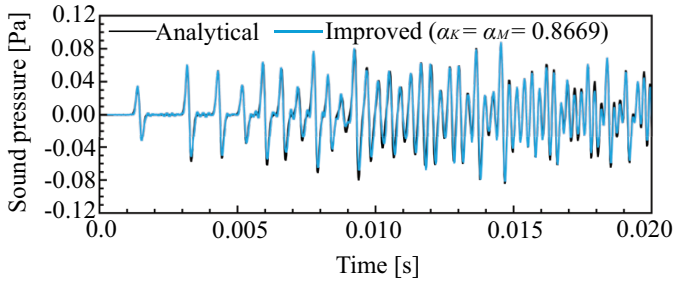

(b) Analytical method vs. TD-FEM using improved Spl27 (α_K= α_M= 0.8669)

Figure 8: Comparison of sound pressures at R3 for FE mesh with λ/d=4.29: (a) Analytical vs. TD-FEM using conventional Spl27 and (b) Analytical vs. TD-FEM using improved Spl27 (α_K=α_M=0.8669).

with

$$e(t) = \sqrt{\frac{1}{N}\frac{\sum_{i=1}^{N}[p_{\text{Ana.}}(\boldsymbol{x}_i,t) - p_{\text{FEM}}(\boldsymbol{x}_i,t)]^2}{\sum_{i=1}^{N} p_{\text{Ana.}}(\boldsymbol{x}_i,t)^2}}, \tag{28}$$

where N_{step} denotes the number of time steps. $p_{\text{Ana.}}(\boldsymbol{x}_i,t)$ and $p_{\text{FEM}}(\boldsymbol{x}_i,t)$ denote sound pressures at receiving point $\boldsymbol{x}_i$ at time t calculated using the analytical method and TD-FEM using conventional and improved Spl27, respectively. Figure 10 presents a comparison of relative errors for all meshes, in which the errors in TD-FEM using improved Spl27 were reduced to 1/2.0–1/3.7 of those in TD-FEM using conventional Spl27 for mesh with same λ/d.

To present further advantages of using the improved Spl27, Figure 11 shows a comparison of mean iteration number of COCG method in TD-FE analysis using conventional and improved Spl27 for each mesh. Results show that mean iteration numbers for improved Spl27 are less than those for conventional Spl27, which means the use of improved Spl27 engenders improvement in convergence property of the iterative method. Including the

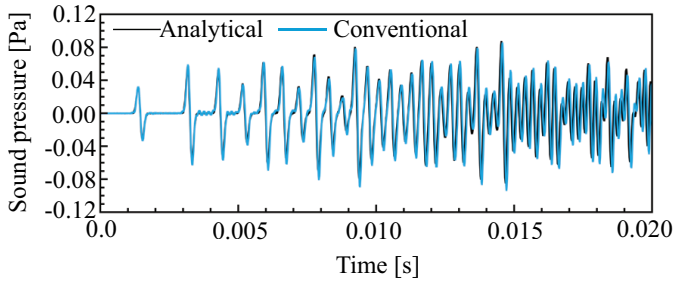

(a) Analytical method vs. TD-FEM using conventional Spl27

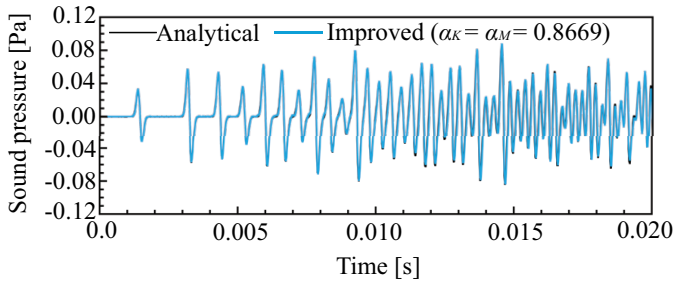

(b) Analytical method vs. TD-FEM using improved Spl27 ($\alpha_K = \alpha_M = 0.8669$)

Figure 9: Comparison of sound pressures at R3 for FE mesh with λ/d=6.0: (a) Analytical vs. TD-FEM using conventional Spl27 and (b) Analytical vs. TD-FEM using improved Spl27 (α_K=α_M=0.8669).

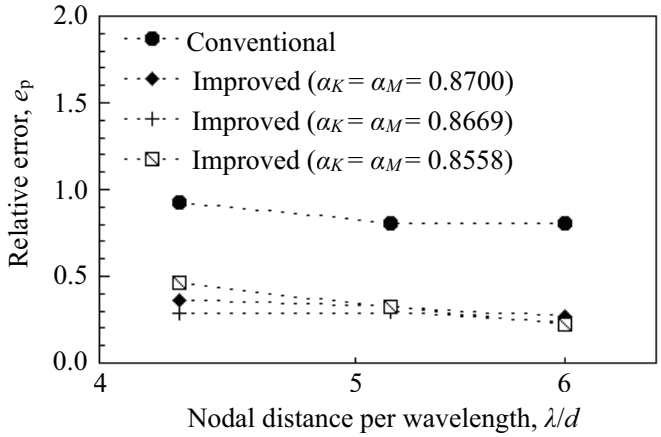

Figure 10: Comparison of relative errors in sound pressure as a function of spatial resolution for TD-FEM using conventional and improved Spl27.

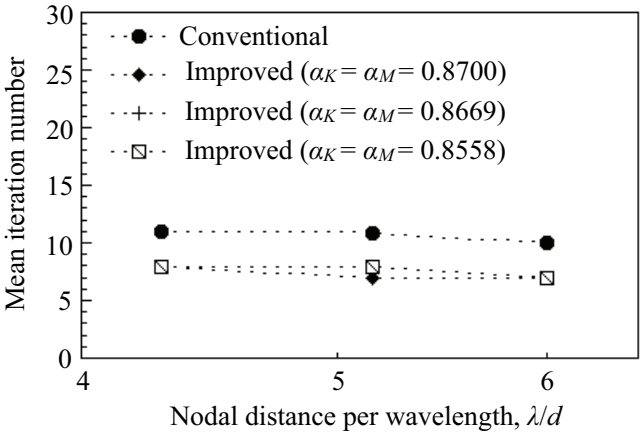

Figure 11: Mean iteration numbers of COCG method as a function of spatial resolution for TD-FEM, obtained using conventional and improved Spl27.

reduction effect of time-step because of the relaxation of stability condition presented above, the reduction rate of number of iterations of 36.5%–43.9% were obtained. Improvement in convergence of the iterative method can also be found for low-order eight-node hexahedral FEs with modified integration points[19].

Results of numerical experiments showed the effectiveness of TD-FEM using improved Spl27 over the conventional method in term of accuracy and computational efficiency for three dimensional analysis.

5. Comparison of accuracy and efficiency of the improved method with those of FEM using conventional hexahedral 27-node elements with Lagrange polynomial function

The accuracy and efficiency of the TD-FEM using improved Spl27 is further demonstrated by comparison with TD-FEM using standard hexahedral 27-node elements with Lagrange polynomial function (Lag27) for a more practical sized room. The sound field in a rectangular room of dimensions of 3 m $\times$ 4 m $\times$ 2.5 m with acoustically rigid boundaries was analyzed using both methods and the computed sound pressures up to 50 ms were compared with analytical solutions. The sound source was located at a position (1.0, 1.0, 1.25) and 69 receiving points were located at (1.0, 0.1–3.5 with 0.1 steps but 1.0 is for source, 1.25) and (2.0, 0.1–3.5 with 0.1 steps, 1.25). The same sound source as that in the previous section was used.

5.1. Setup of FE analysis

The rectangular room was discretized by rectangular elements and spatial resolution $\lambda/d_{\max}$ of the mesh with DOF of 9,783,015 is 5.64 at 4 kHz, where $d_{\max}$ is the maximum nodal distance. Three modified integration points presented in the previous section were used for the improved Spl27. The time intervals Δt's for TD-FEM using improved Spl27 and Lag27 are, respectively, 1/47,000 s and 1/65,000 s, where the critical time intervals are, respectively, 1/45,725 s (α_K=α_M=0.8700), 1/45,947 s (α_K=α_M=0.8669), 1/46,759 s (α_K=α_M=0.8558) and 1/64,537 s (Lag27). Here, it was presented that the larger time interval is available for the improved method.

5.2. Results and discussions

Figure 12 shows sound pressures at a position (2.0, 3.5, 1.25) calculated using the analytical method and TD-FEM using improved Spl27 (α_K=α_M=0.8669) and Lag27. A fine structure of sound pressure calculated using TD-FEM using improved Spl27 agrees well with that calculated using an analytical solution, whereas numerical oscillation is observed for sound pressure calculated using TD-FEM using Lag27. The relative errors from an analytical solution for TD-FEM using both improved Spl27 and Lag27 are, respectively, 0.032(α_K=α_M=0.8700), 0.028 (α_K=α_M=0.8669), 0.028 (α_K=α_M=0.8558) and 0.086 (Lag27). Furthermore, the mean iteration numbers for both methods are, respectively, 6.98 (α_K=α_M=0.8700), 7.0 (α_K=α_M=0.8669), 7.1 (α_K=α_M=0.8558) and 11.2 (Lag27). Including the effect of reduction of time steps, reduction rates of number of iteration of 54.3–54.8% were obtained. These results underscore the effectiveness of TD-FEM using improved Spl27 over that using Lag27.

6. Conclusions

For efficient room acoustics simulation with complicated boundary conditions at higher frequencies, this paper presented an FEM using the improved Spl27 that uses modified integration points in numerical integrations of element matrices based on dispersion relation in one dimension. Here, we specifically examined reduction of only spatial discretization error. The basic accuracy and computational efficiency over FEM using conventional Spl27 and Lag27 were tested through numerical experiments in three dimensions, where frequencies up to 4 kHz were analyzed. Numerical experiments using benchmark problems in both frequency and time domains showed that FEM

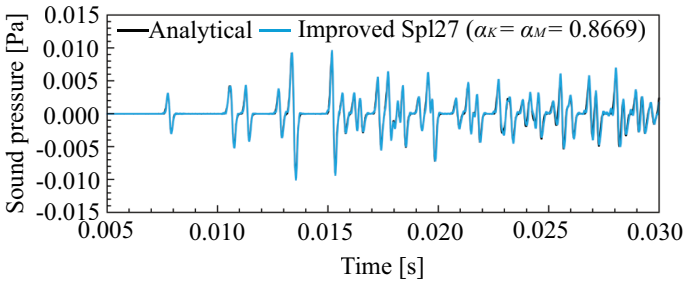

(a) Analytical method vs. TD-FEM using improved Spl27 ($\alpha_K = \alpha_M = 0.8669$)

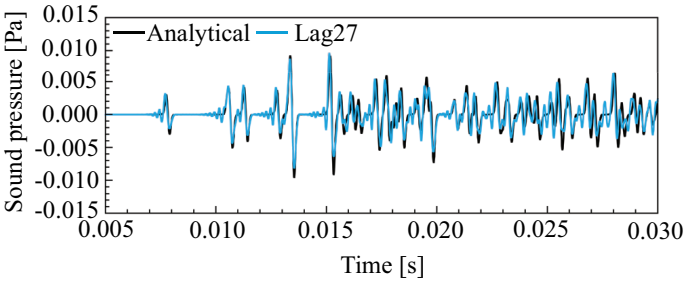

(b) Analytical method vs. TD-FEM using Lag27

Figure 12: Sound pressures at (2.0, 3.5, 1.25) obtained from the analytical method and TD-FEM using both elements: (a) Analytical vs. TD-FEM using improved Spl27 (α_K=α_M=0.8669) and (b) Analytical vs. TD-FEM using Lag27.

using the improved Spl27 provides more accurate results than FEM using conventional Spl27 in both domains, on the FE meshes with the same spatial resolution. We also showed additional advantages using improved Spl27, i.e., relaxation effect of stability condition and improvement in convergence of an iterative method, for time domain analysis. Furthermore, a numerical experiment with a practical sized room showed TD-FEM using improved Spl27 performs better than that using Lag27 with fewer time steps and with a better convergence property of the iterative method.

As the results showed, it can be concluded that the presented FEM enables us to predict sound fields of rooms at the high-frequency region more accurately than conventional methods can, and with a lower computational cost.

As a subject of future study, it might be possible to reduce the dispersion error further by modifying both numerical integration points and weights in numerical integration process. Application of the improved method to sound field analysis with complicated geometry and with finite impedance

boundary conditions is also a subject of future research.

Acknowledgement

This research was partially supported by the Research Fund at the Discretion of the President of Oita University and by a Grant-in-Aid for Science Research (B) 24360238 from the Japan Society for the Promotion of Science.

References

[1] Choi S, Tachibana H, Estimation of impulse response in a room by the finite element method, J Acoust Soc Jpn 1993; 49(5):328–33.(in Japanese)

[2] Otsuru T, Fujii K, Finite elemental analysis of sound field in rooms with sound absorbing materials, Proc Inter-noise 1994; 94:2011–4.

[3] Easwaran V, Craggs A, Transient response of lightly damped rooms: a finite element approach, J Acoust Soc Am 1996; 99(1):108–13.

[4] Easwaran V, Craggs A, An application of acoustic finite element models to finding the reverberation times of irregular rooms, Acoust Acta Acoust 1996; 82:54–64.

[5] Otsuru T, Uchinoura Y, Tomiku R, Okamoto N, Takahashi Y, Basic concept, accuracy and application of large-scale finite element sound field analysis of rooms, Proc. 18th International Congress on Acoustics 2004 on CD-ROM(Mo5.B2.2); 2004.

[6] Okamoto N, Tomiku R, Otsuru T, Yasuda Y, Numerical analysis of large-scale sound fields using iterative methods part II: application of Krylov subspace methods to finite element analysis, J Comp Acoust 2007; 15(4):473–93.

[7] Okuzono T, Otsuru T, Okamoto N, Tomiku R, Sound field analysis of rooms by time domain finite element method with an iterative method, J Environ Eng(Trans AIJ) 2008; 628:701–6.(in Japanese)

[8] Okuzono T, Sueyoshi T, Otsuru T, Okamoto N, Tomiku R, Time domain finite element sound field analysis of rooms using iterative methods and parallelization, Proc Inter-noise 2006 on CD-ROM(in06_401); 2006.

[9] Okuzono T, Otsuru T, Tomiku R, Okamoto N, Minokuchi T, Speedup of time domain finite element sound field analysis of rooms, Proc Internoise 2008 on CD-ROM(0877); 2008.

[10] Otsuru T, Tomiku R, Basic characteristics and accuracy of acoustic element using spline function in finite element sound field analysis, Acoust Sci Technol 2000; 21(2):87–95.

[11] Marburg S, Nolte B, Computational acoustics of noise propagation in fluids-finite and boundary element methods, Springer; 2008.

[12] Tomiku R, Otsuru T, Sound fields analysis in an irregular-shaped reverberation room by finite element method, J Archit Plann Environ Eng 2002; 551:9–15.(in Japanese)

[13] Otsuru T, Okuzono T, Okamoto N, Isobe K, Furuya H, Time domain large-scale finite element sound field analysis of a multi-purpose hall, Proc. the 14th International Congress on Sound and Vibration on CD-ROM(P440); 2007.

[14] Okuzono T, Otsuru T, Tomiku R, Okamoto N, Fundamental accuracy of time domain finite element method for sound-field analysis of rooms, Appl Acoust 2010; 71(10):940–6.

[15] LL Thompson, A review of finite-element methods for time-harmonic acoustics, J Acoust Soc Am 2006; 119(3):1315–30.

[16] B Yue, MN Guddati, Dispersion-reducing finite elements for transient acoustics, J Acoust Soc Am 2005; 118(4):2132–41.

[17] S Krenk, Dispersion-corrected explicit integration of the wave equation, Comput Methods Appl Mech Engrg 2001; 191:975–87.

[18] MN Guddati, B Yue, Modified integration rules for reducing dispersion error in finite element methods, Comput Methods Appl Mech Engrg 2004; 193:275–87.

[19] Okuzono T, Otsuru T, Tomiku R, Okamoto N, Application of modified integration rule to time-domain finite-element acoustic simulation of rooms, J Acoust Soc Am 2012; 132(2):804–13.

[20] Newmark NM, A method of computation for structural dynamics, J Eng Mech Div 1959; 85:67–94.

[21] Hughes TJR, The finite element method linear static and dynamic finite element analysis, Dover; 2000.

[22] Okuzono T, Otsuru T, Tomiku R, Okamoto N, Dispersion-reduced spline acoustic finite elements for frequency-domain analysis, Acoust Sci Technol 2013 (accepted for publication).

[23] Otsuru T, Sakuma T, Sakamoto S, Constructing a database of computational methods for environmental acoustics, Acoust Sci Technol 2005; 26:221–4.

[24] van der Vorst HA, Melissen J, A Petrov-Galerkin type method for solving $Ax{=}b$, where A is symmetric complex, IEEE Trans Magn 1990; 26(2):706–8.

[25] Sakamoto S, Phase-error analysis of high-order finite difference time-domain scheme and its influence on calculation results of impulse response in closed sound field, Acoust Sci Technol 2007; 28(5):295–309.